Hydrothermal Synthesis and Structural Characterization of Mixed-Valence Iron Phosphates: $AFe_5(PO_4)_5(OH)\cdot H_2O$ (A = Ca, Sr)

Edita Dvoncova and Kwang-Hwa Lii*

Institute of Chemistry, Academia Sinica, Nankang, Taipei, Taiwan, Republic of China

Received April 8, 1993®

Mixed-valence iron phosphates of the stoichiometry $AFe_5(PO_4)_5(OH)\cdot H_2O$ (A = Ca, Sr) have been synthesized hydrothermally and structurally characterized by single-crystal X-ray diffraction. Crystal data: $CaFe_5(PO_4)_5(OH)\cdot H_2O$, triclinic, $P\bar{1}$, a = 6.404(1) Å, b = 7.866(1) Å, c = 15.694(2) Å, α = 85.00(1)°, β = 88.79(1)°, γ = 78.22(1)°, V = 770.97(18) Å^3, Z = 2, R = 0.034 for 2544 unique reflections; $SrFe_5(PO_4)_5(OH)\cdot H_2O$, triclinic, $P\bar{1}$, a = 6.4303(2) Å, b = 7.8749(8) Å, c = 15.894(2) Å, α = 84.75(1)°, β = 87.96(1)°, γ = 78.114(9)°, V = 784.16(16) Å^3, Z = 2, R = 0.0469 for 1854 unique reflections. The two compounds are isostructural. The complex framework consists of dimers of corner-sharing and edge-sharing $Fe^{III}O_6$ octahedra joined through $Fe^{II}O_5$ trigonal bipyramids by corner- and edge-sharing, and discrete $Fe^{III}O_6$ octahedra. Phosphate tetrahedra further knit together these Fe–O polyhedra by corner-sharing. Schlegel diagrams are used to help describe the arrangement of the next-nearest neighbors of the coordination polyhedra of Fe. The calcium ions are 7-coordinated and are located at intersections of the tunnels along the [010] and [110] directions. The structures are further defined by thermogravimetric and Mossbauer studies. Mossbauer spectroscopy confirms the presence of one Fe^{II} and four Fe^{III} ions.

Introduction

Iron phosphates have shown a rich structural chemistry owing to the accessibility of more than one iron oxidation state and the ability of iron–oxygen polyhedra and phosphate tetrahedra to form a variety of complex network structures. Basic iron phosphates exist as minerals and are considered as among the most perplexing substances in the mineral kingdom.[1] These interesting compounds present a challenge to complete structural characterization from a basic research point of view. The preparation of single crystals of iron phosphates calls upon several methods: hydrothermal growth, fluoride flux, vapor-phase transport with $FeCl_2$, or simply prolonged heating. In the course of a general survey of novel structures of transition metal phosphates, we have recently synthesized and structurally characterized several new compounds in ternary vanadium or iron phosphate systems by hydrothermal techniques. Hydrothermal synthesis involves the use of aqueous solvents or mineralizers under high temperature and high pressure to dissolve and recrystallize materials that are relatively insoluble under ordinary conditions. Several new compounds in the iron system have been synthesized: $AFeP_2O_7$ (A = Rb, Cs),[2] $SrFe_3(PO_4)_3(HPO_4)$,[3] $CaFe_2(PO_4)_2(HPO_4)$,[4] and $AFe_3(P_2O_7)_2$ (A = Sr, Ba).[5] The structures of these iron phosphates cover discrete FeO_6 octahedra, FeO_5 trigonal bipyramids, dimers of face-sharing or edge-sharing FeO_6 octahedra, and infinite chains of FeO_6 octahedra sharing either trans or skew edges. They include ferric and ferrous compounds. We have now prepared two novel mixed-valence iron phosphates, $AFe_5(PO_4)_5(OH)\cdot H_2O$ (A = Ca, Sr), whose complex framework consists of dimers of corner-sharing and edge-sharing $Fe^{III}O_6$ octahedra, joined through $Fe^{III}O_5$ trigonal bipyramids by corner- and edge-sharing, and discrete $Fe^{III}O_6$ octahedra. We report here the synthesis, single-crystal X-ray structures, thermal analysis, and Mossbauer spectroscopy of $AFe_5(PO_4)_5(OH)\cdot H_2O$ (A = Ca, Sr).

Experimental Section

Synthesis. Hydrothermal reactions were performed in a gold-lined Morey-type closure autoclave (5.5 cm × 2 cm inside diameter) with an internal volume of 16 mL. A reaction mixture of $Ca(OH)_2$ (0.1850 g), FeO (0.1794 g), $FePO_4$ (1.5060 g) (molar ratio 1:1:4) and 3.75 M H_3PO_4(aq) (8 mL) was heated at 400 °C for 2.5 d followed by cooling to room temperature in 8 h. Upon opening of the autoclave, it was found that the product contained greenish-black plate-shaped crystals of $CaFe_5(PO_4)_5(OH)\cdot H_2O$. Powder X-ray diffraction using a Rigaku powder diffractometer on the bulk product confirmed its purity for subsequent Mossbauer spectroscopy and thermal analysis. The yield was 84% based on iron.

The crystal growth of $SrFe_5(PO_4)_5(OH)\cdot H_2O$ was achieved by heating a reaction mixture of $Sr(OH)_2\cdot 8H_2O$ (0.6634 g), FeO (0.1794 g), $FePO_4$ (1.5060 g) (molar ratio 1:1:4), and 3.75 M H_3PO_4 (8 mL) at 400 °C for 2.5 days. Besides the greenish-black crystals of the required compound, the product also contained tan crystals of $SrFe_3(PO_4)_3(HPO_4)$[3] and much green polycrystalline material.

The compositions deduced from the structure determination of $CaFe_5(PO_4)_5(OH)\cdot H_2O$ and $SrFe_5(PO_4)_5(OH)\cdot H_2O$ were checked by energy dispersive X-ray fluorescence analysis (EDX) which gave an A:Fe:P molar ratio (A = Ca, Sr) equal to 0.9:5.4:5.1 and 1:4.8:5.2 for the Ca and Sr compounds, respectively. $CaFe_5(PO_4)_5(OH)\cdot H_2O$ was further characterized by thermogravimetric analysis under N_2 using a DuPont thermal analyzer. It began to decompose at ~550 °C and exhibited a weight loss of 3.12% at 900 °C. The weight loss corresponds to the loss of 1.5 water molecule and can be compared with the calculated value of 3.26%. An experiment was performed in which $CaFe_5(PO_4)_5(OH)\cdot H_2O$ was heated in flowing N_2 at 900 °C for 16 h. The X-ray powder pattern of the product of this heat treatment has not been successfully indexed.

Single-Crystal X-ray Diffraction Study. Two small greenish black crystals having dimensions of 0.01 × 0.05 × 0.25 mm for $CaFe_5(PO_4)_5(OH)\cdot H_2O$ and 0.01 × 0.05 × 0.12 mm for $SrFe_5(PO_4)_5(OH)\cdot H_2O$ were selected for indexing and intensity data collection on an Enraf-Nonius CAD4 diffractometer with κ-axis geometry using graphite-monochromated Mo Kα radiation at 23 °C. Axial oscillation photographs along the three axes were taken to check the unit cell parameters. Octants collected: $+h,\pm k,\pm l$ for $CaFe_5(PO_4)_5(OH)\cdot H_2O$; $+h,\pm k,\pm l$ for $SrFe_5(PO_4)_5(OH)\cdot H_2O$. Of the 3334 (3874) reflections collected 2544 (1854) unique reflections were considered observed ($I > 2.5\sigma(I)$) after Lorentz polarization and empirical absorption corrections for $CaFe_5(PO_4)_5(OH)\cdot H_2O$ and $SrFe_5(PO_4)_5(OH)\cdot H_2O$, respectively. Correction for absorption was based on ψ scans of a few suitable reflections with χ values close to 90° ($T_{min/max}$ = 0.825/0.999, 0.754/0.998 for the Ca and Sr compounds, respectively). On the basis of the statistical analysis of the intensity data and successful solution and refinement of the structures,

* To whom correspondence should be addressed.
® Abstract published in *Advance ACS Abstracts*, August 15, 1993.

(1) Moore, P. B. *Am. Mineral.* **1970**, *55*, 135.
(2) Dvoncova, E.; Lii, K. H. *J. Solid. State Chem.* **1993**, *105*, 279.
(3) Lii, K. H.; Dong, T. Y.; Cheng, C. Y.; Wang, S. L. *J. Chem. Soc., Dalton Trans.* **1993**, 577.
(4) Lii, K. H. Unpublished research.
(5) Lii, K. H.; Shih, P. F.; Chen, T. M. *Inorg. Chem.*, following paper in this issue.

0020-1669/93/1332-4368$04.00/0

Table I. Crystallographic Data for $CaFe_5(PO_4)_5(OH)\cdot H_2O$ and $SrFe_5(PO_4)_5(OH)\cdot H_2O$

formula	$CaFe_5H_3O_{22}P_5$	$Fe_5H_3O_{22}P_5Sr$
fw	829.19	876.73
space group	$P\bar{1}$ (No. 2)	$P\bar{1}$ (No. 2)
a, Å	6.404(1)	6.4303(2)
b, Å	7.866(1)	7.8749(8)
c, Å	15.694(2)	15.894(2)
α, deg	85.00(1)	84.75(1)
β, deg	88.79(1)	87.96(1)
γ, deg	78.22(1)	78.114(9)
V, Å^3	770.97(18)	784.16(16)
Z	2	2
T, °C	23	23
λ, Å	0.709 30	0.709 30
ρ_{calc}, g/cm^3	3.572	3.713
μ, cm^{-1}	55.8	85.2
$2\theta_{max}$, deg	55	55
R^a	0.0340	0.0469
R_w^b	0.0370	0.0485

^{a} $R = \sum||F_o| - |F_c||/|F_o|$. ^{b} $R_w = [\sum w(|F_o| - |F_c|)^2/\sum w|F_o|^2]^{1/2}$; $w^{-1} = \sigma^2(F) + gF^2$.

the space groups for both compounds were determined to be $P\bar{1}$. Direct methods were used to locate the metal atoms with the remaining non-hydrogen atoms being found from successive difference maps. For $CaFe_5(PO_4)_5(OH)\cdot H_2O$ all atoms were refined with anisotropic temperature factors. For $SrFe_5(PO_4)_5(OH)\cdot H_2O$ we earlier attempted anisotropic displacement parameter refinement, but several oxygen atoms converged to nonpositive definite values and the data to parameter ratio was too low, and therefore we decided to remain in the isotropic mode for the oxygen atoms. On the basis of bond-length bond-strength calculations, Fe(2) is divalent, other Fe atoms are trivalent, two of the oxygen atoms were found to be considerably undersaturated, and all other oxygen atoms have bond valence sums very close to 2.0. Further support of the calculation results is gained by the dark green color of the crystals, a phenomenon indicative of mixed-valence states of iron in the crystal. In order to balance the charge, three hydrogen atoms must be included in the formula. Valence sums of 1.02 (1.03) and 0.43 (0.38) were calculated for O(11) and O(20) for the Ca and Sr compounds, respectively. The value for O(20) is typically associated with the presence of two hydrogen atoms. The other value suggests that O(11) is bonded to a hydrogen atom. The positions of the protons in the Ca compound could be inferred from the O···O distances not involved in the coordination polyhedra: there is a short one (2.630 Å) between O(11) and O(2), which presumably involves the proton on O(11); there is O(20)···O(18), at 2.793 Å, and O(20)···O(19), at 2.995 Å, to accommodate the two H atoms on O(20). However, the necessary three hydrogen atoms could not be located from a different Fourier map. The final cycles of full-matrix least-squares refinement converged at $R = 0.034$ and $R_w = 0.037$ for $CaFe_5(PO_4)_5(OH)\cdot H_2O$ and $R = 0.047$ and $R_w = 0.048$ for $SrFe_5(PO_4)_5(OH)\cdot H_2O$. In the final difference Fourier map the deepest hole was -0.80 e/Å^3 (-1.11 e/Å^3) and the highest peak 0.96 e/Å^3 (1.17 e/Å^3) for the Ca and the Sr compounds, respectively. Neutral-atom scattering factors for all atoms were used. Anomalous dispersion corrections were applied. No secondary extinction correction was performed. Calculations were performed on a DEC MicroVAX computer system using SHELXTL-Plus programs.[6]

Mossbauer Spectroscopy. The ^{57}Fe Mossbauer spectrum of $CaFe_5(PO_4)_5(OH)\cdot H_2O$ was measured on a constant-acceleration instrument. Velocity calibrations were made using 99.99% pure 10-μm iron foil. Typical line widths for all three pairs of iron lines fell in the range 0.28–0.30 mm/s. Isomer shifts are reported with respect to iron foil at 300 K. It should be noted that the isomer shifts illustrated are plotted as experimentally obtained; tabulated data should be consulted.

Results and Discussion

Structure. The crystallographic data are listed in Table I. The atomic coordinates, thermal parameters, and selected bond distances and bond valence sums[7] are listed in Tables II and III. All atoms are located at general positions. The iron atoms are five- or six-coordinated. The coordination numbers of alkaline-earth metals were determined on the basis of the maximum gap in the metal–oxygen distances ranked in increasing distances. Both Ca and Sr are coordinated by seven oxygen atoms, and the

Table II. Atomic Positions and Thermal Parameters (Å^2 × 100) for $CaFe_5(PO_4)_5(OH)\cdot H_2O$ and $SrFe_5(PO_4)_5(OH)\cdot H_2O$

atom	x	y	z	U_{eq}^a
		$CaFe_5(PO_4)_5(OH)\cdot H_2O$		
Ca	0.0228(2)	0.3974(1)	0.14159(7)	1.12(3)
Fe(1)	0.0398(1)	0.7918(1)	0.48662(5)	0.66(2)
Fe(2)	0.4025(1)	0.5943(1)	0.62443(5)	0.95(2)
Fe(3)	0.3926(1)	0.1294(1)	0.29002(5)	0.67(2)
Fe(4)	0.2787(1)	0.2785(1)	0.75078(5)	0.66(2)
Fe(5)	0.2857(1)	0.7677(1)	0.00548(5)	0.68(2)
P(1)	0.0848(2)	0.9480(2)	0.68091(8)	0.60(4)
P(2)	0.0832(2)	0.4718(2)	0.36061(8)	0.51(4)
P(3)	–0.4655(2)	0.7984(2)	0.43632(8)	0.59(4)
P(4)	–0.2157(2)	0.8116(2)	0.04670(8)	0.59(4)
P(5)	–0.5142(2)	0.4418(2)	0.14925(8)	0.62(4)
O(1)	0.0139(6)	0.9791(5)	0.5845(2)	0.80(11)
O(2)	–0.0727(6)	0.3766(5)	0.4127(2)	0.90(11)
O(3)	0.1215(6)	0.6252(5)	0.4041(2)	1.14(11)
O(4)	0.6266(6)	0.2560(5)	0.4980(2)	0.87(11)
O(5)	0.3022(6)	0.8190(5)	0.6889(2)	0.88(11)
O(6)	0.3010(6)	0.3483(5)	0.3504(2)	0.71(10)
O(7)	0.4166(6)	0.3338(5)	0.6341(2)	0.89(11)
O(8)	–0.0833(6)	0.8678(5)	0.7330(2)	0.86(11)
O(9)	0.5619(6)	0.0264(5)	0.6096(2)	1.11(11)
O(10)	0.3787(6)	0.2903(5)	0.1844(2)	0.79(11)
O(11)^b	0.4963(6)	0.0644(5)	0.7857(2)	1.07(11)
O(12)	–0.0209(6)	0.5262(5)	0.2725(2)	0.79(11)
O(13)	0.1633(6)	0.2978(5)	0.8672(2)	1.07(11)
O(14)	0.5535(6)	0.5346(5)	0.2224(2)	1.01(11)
O(15)	0.1037(6)	0.1196(5)	0.7145(2)	1.14(11)
O(16)	–0.2589(6)	0.7963(5)	0.4822(2)	1.13(11)
O(17)	–0.4180(6)	0.7793(5)	0.0089(2)	1.23(12)
O(18)	0.2322(6)	0.9978(5)	–0.0644(2)	1.11(11)
O(19)	–0.0262(6)	0.7494(5)	–0.0129(2)	0.96(11)
O(20)^c	0.1973(7)	0.9078(6)	0.1106(3)	1.66(13)
O(21)	0.3151(6)	0.5591(5)	0.0908(2)	1.09(11)
O(22)	0.3145(6)	0.6334(5)	–0.0978(2)	0.91(11)
		$SrFe_5(PO_4)_5(OH)\cdot H_2O$		
Sr	0.0231(2)	0.3851(2)	0.14258(8)	1.27(4)
Fe(1)	0.0371(3)	0.7913(2)	0.4872(2)	0.77(6)
Fe(2)	0.3973(3)	0.5950(2)	0.6221(1)	1.02(6)
Fe(3)	0.4008(3)	0.1305(2)	0.2929(1)	0.74(5)
Fe(4)	0.2721(3)	0.2768(2)	0.7480(1)	0.73(5)
Fe(5)	0.2952(3)	0.7667(2)	0.0099(1)	0.71(5)
P(1)	0.0787(5)	0.9480(4)	0.6776(2)	0.78(10)
P(2)	0.0876(5)	0.4738(4)	0.3621(2)	0.73(10)
P(3)	–0.4645(5)	0.7976(4)	0.4367(2)	0.62(9)
P(4)	–0.2119(5)	0.8165(4)	0.0500(2)	0.75(10)
P(5)	–0.5080(5)	0.4426(4)	0.1499(2)	0.58(9)
O(1)	0.011(1)	0.981(1)	0.5815(5)	0.54(17)
O(2)	–0.070(1)	0.375(1)	0.4130(6)	1.03(19)
O(3)	0.126(1)	0.626(1)	0.4061(6)	1.11(19)
O(4)	0.631(1)	0.254(1)	0.4982(6)	0.96(18)
O(5)	0.298(1)	0.817(1)	0.6858(6)	1.22(19)
O(6)	0.305(1)	0.351(1)	0.3509(5)	0.58(17)
O(7)	0.417(1)	0.333(1)	0.6339(5)	0.87(18)
O(8)	–0.092(1)	0.869(1)	0.7277(6)	1.05(19)
O(9)	0.559(1)	0.026(1)	0.6076(6)	1.05(19)
O(10)	0.396(1)	0.290(1)	0.1873(5)	0.75(18)
O(11)^b	0.490(1)	0.061(1)	0.7815(6)	0.94(18)
O(12)	–0.015(1)	0.533(1)	0.2770(5)	0.69(17)
O(13)	0.157(2)	0.282(1)	0.8626(6)	1.38(20)
O(14)	0.577(1)	0.529(1)	0.2191(6)	1.11(19)
O(15)	0.098(1)	0.118(1)	0.7098(6)	1.23(20)
O(16)	–0.259(1)	0.793(1)	0.4802(6)	1.06(19)
O(17)	–0.405(2)	0.769(1)	0.0145(6)	1.53(20)
O(18)	0.254(1)	0.989(1)	–0.0625(6)	1.09(19)
O(19)	–0.015(1)	0.757(1)	–0.0060(6)	1.02(19)
O(20)^c	0.203(2)	0.914(1)	0.1149(6)	1.80(21)
O(21)	0.315(1)	0.564(1)	0.0981(6)	0.98(19)
O(22)	0.325(1)	0.626(1)	–0.0895(5)	0.87(18)

^{a} U_{eq} is defined as one-third of the trace of the orthogonalized U_{ij} tensor. ^{b} Hydroxyl oxygen atom. ^{c} Water oxygen atom.

(6) Sheldrick, G. M. SHELXTL-PLUS *Crystallographic System, Release 4.11*; Siemens Analytical X-Ray Instruments Inc.: Madison, WI, 1990.
(7) Brown, I. D.; Altermatt, D. *Acta Crystallogr.* **1985**, *B41*, 244.

Table III. Bond Lengths (Å) and Bond Valence Sums ($\sum s$) for $CaFe_5(PO_4)_5(OH)\cdot H_2O$ and $SrFe_5(PO_4)_5(OH)\cdot H_2O$

$CaFe_5(PO_4)_5(OH)\cdot H_2O$				$SrFe_5(PO_4)_5(OH)\cdot H_2O$			
Ca–O(8)	2.713(4)	Ca–O(10)	2.354(4)	Sr–O(8)	2.718(8)	Sr–O(19)	2.540(9)
Ca–O(12)	2.356(4)	Ca–O(13)	2.444(4)	Sr–O(10)	2.468(9)	Sr–O(21)	2.611(10)
Ca–O(19)	2.409(4)	Ca–O(21)	2.547(4)	Sr–O(12)	2.507(9)	Sr–O(22)	2.440(9)
Ca–O(22)	2.346(4)			Sr–O(13)	2.632(8)		
$\sum s$(Ca–O) = 1.98				$\sum s$(Sr–O) = 2.19			
Fe(1)–O(1)	2.201(4)	Fe(1)–O(3)	1.911(4)	Fe(1)–O(1)	2.188(9)	Fe(1)–O(3)	1.902(9)
Fe(1)–O(1)	2.006(4)	Fe(1)–O(4)	2.107(4)	Fe(1)–O(1)	1.992(9)	Fe(1)–O(4)	2.108(10)
Fe(1)–O(2)	1.958(4)	Fe(1)–O(16)	1.909(4)	Fe(1)–O(2)	1.951(8)	Fe(1)–O(16)	1.909(10)
$\sum s$(Fe(1)–O) = 3.12				$\sum s$(Fe(1)–O) = 3.18			
Fe(2)–O(2)	2.164(4)	Fe(2)–O(6)	2.092(4)	Fe(2)–O(2)	2.154(10)	Fe(2)–O(6)	2.112(9)
Fe(2)–O(4)	2.156(4)	Fe(2)–O(7)	2.025(4)	Fe(2)–O(4)	2.148(9)	Fe(2)–O(7)	2.034(9)
Fe(2)–O(5)	2.094(4)			Fe(2)–O(5)	2.079(9)		
$\sum s$(Fe(2)–O) = 1.85				$\sum s$(Fe(2)–O) = 1.85			
Fe(3)–O(5)	2.114(4)	Fe(3)–O(9)	1.899(4)	Fe(3)–O(5)	2.108(10)	Fe(3)–O(9)	1.906(9)
Fe(3)–O(6)	2.014(4)	Fe(3)–O(10)	1.987(4)	Fe(3)–O(6)	2.012(8)	Fe(3)–O(10)	1.998(8)
Fe(3)–O(8)	2.016(4)	Fe(3)–O(11)	2.020(4)	Fe(3)–O(8)	2.022(10)	Fe(3)–O(11)	2.001(9)
$\sum s$(Fe(3)–O) = 3.10				$\sum s$(Fe(3)–O) = 3.10			
Fe(4)–O(7)	2.067(4)	Fe(4)–O(13)	1.963(4)	Fe(4)–O(7)	2.062(9)	Fe(4)–O(13)	1.942(10)
Fe(4)–O(11)	1.998(4)	Fe(4)–O(14)	2.065(4)	Fe(4)–O(11)	2.009(8)	Fe(4)–O(14)	2.086(10)
Fe(4)–O(12)	2.027(4)	Fe(4)–O(15)	1.966(4)	Fe(4)–O(12)	2.012(8)	Fe(4)–O(15)	1.988(10)
$\sum s$(Fe(4)–O) = 3.03				$\sum s$(Fe(4)–O) = 3.02			
Fe(5)–O(17)	1.921(4)	Fe(5)–O(20)	2.069(4)	Fe(5)–O(17)	1.935(11)	Fe(5)–O(20)	2.118(10)
Fe(5)–O(18)	2.003(4)	Fe(5)–O(21)	2.006(4)	Fe(5)–O(18)	1.978(8)	Fe(5)–O(21)	2.011(8)
Fe(5)–O(19)	2.060(4)	Fe(5)–O(22)	1.996(4)	Fe(5)–O(19)	2.038(10)	Fe(5)–O(22)	1.992(9)
$\sum s$(Fe(5)–O) = 3.08				$\sum s$(Fe(5)–O) = 3.06			
P(1)–O(1)	1.572(4)	P(1)–O(8)	1.541(4)	P(1)–O(1)	1.586(9)	P(1)–O(8)	1.536(10)
P(1)–O(5)	1.547(4)	P(1)–O(15)	1.520(4)	P(1)–O(5)	1.564(9)	P(1)–O(15)	1.504(10)
$\sum s$(P(1)–O) = 4.86				$\sum s$(P(1)–O) = 4.84			
P(2)–O(2)	1.546(4)	P(2)–O(6)	1.542(4)	P(2)–O(2)	1.563(10)	P(2)–O(6)	1.543(8)
P(2)–O(3)	1.501(4)	P(2)–O(12)	1.535(4)	P(2)–O(3)	1.510(10)	P(2)–O(12)	1.519(9)
$\sum s$(P(2)–O) = 5.05				$\sum s$(P(2)–O) = 5.02			
P(3)–O(4)	1.539(4)	P(3)–O(9)	1.516(4)	P(3)–O(4)	1.553(10)	P(3)–O(9)	1.514(8)
P(3)–O(7)[b]	1.566(4)	P(3)–O(16)	1.516(5)	P(3)–O(7)	1.569(9)	P(3)–O(16)	1.504(10)
$\sum s$(P(3)–O) = 5.01				$\sum s$(P(3)–O) = 5.01			
P(4)–O(13)	1.541(4)	P(4)–O(18)	1.530(4)	P(4)–O(13)	1.544(9)	P(4)–O(18)	1.532(9)
P(4)–O(17)	1.513(5)	P(4)–O(19)	1.542(4)	P(4)–O(17)	1.512(11)	P(4)–O(19)	1.537(9)
$\sum s$(P(4)–O) = 5.04				$\sum s$(P(4)–O) = 5.04			
P(5)–O(10)	1.548(4)	P(5)–O(21)	1.539(4)	P(5)–O(10)	1.529(9)	P(5)–O(21)	1.539(9)
P(5)–O(14)	1.528(4)	P(5)–O(22)	1.539(4)	P(5)–O(14)	1.517(10)	P(5)–O(22)	1.535(9)
$\sum s$(P(5)–O) = 4.95				$\sum s$(P(5)–O) = 5.06			

eighth distances are at 3.249 and 3.108 Å, respectively. Bond valence sums for all cations are in good accordance with their formal oxidation states. Since the two compounds are isostructural, only the calcium compound will be discussed in the following.

$CaFe_5(PO_4)_5(OH)\cdot H_2O$ adopts a new structural type. Figure 1 is a polyhedral diagram projected down the [100] direction. The structure consists of edge-sharing dimers of composition $Fe(1)_2O_{10}$, corner-sharing dimers of composition $Fe(3)Fe(4)(OH)O_{10}$, discrete $Fe(5)O_5(H_2O)$ octahedra, $Fe(2)O_5$ trigonal bipyramids, and PO_4 tetrahedra. The edge-sharing dimers sit on inversion centers. The hydroxyl oxygen, O(11), of $Fe(3)Fe(4)(OH)O_{10}$ is the bridging atom. These dimers are joined by $Fe(2)O_5$ trigonal bipyramids to form the denser part of the framework. The P(1), P(2), and P(3) tetrahedra further knit together these Fe polyhedra by corner-sharing. Discrete Fe(5) octahedra are connected to each other and to the denser part of the framework by corner-sharing P(4) and P(5) tetrahedra. The P–O bond lengths have average values of 1.545 Å for P(1) and 1.531–1.538 Å for other P atoms. The value for P(1) is somewhat greater than the expected value of 1.53 Å predicted by Shannon[8] for phosphate structures where the coordination number for phosphate oxygen atoms is 3. The Ca^{2+} ions are located at intersections of the tunnels along [010] and [110] near discrete Fe(5) octahedra. Each calcium ion is coordinated to 7 phosphate oxygen atoms. The configuration is approximately that of a trigonal prism with the seventh oxygen O(8) approaching at one tetragonal face. The configuration of SrO_7 is similar.

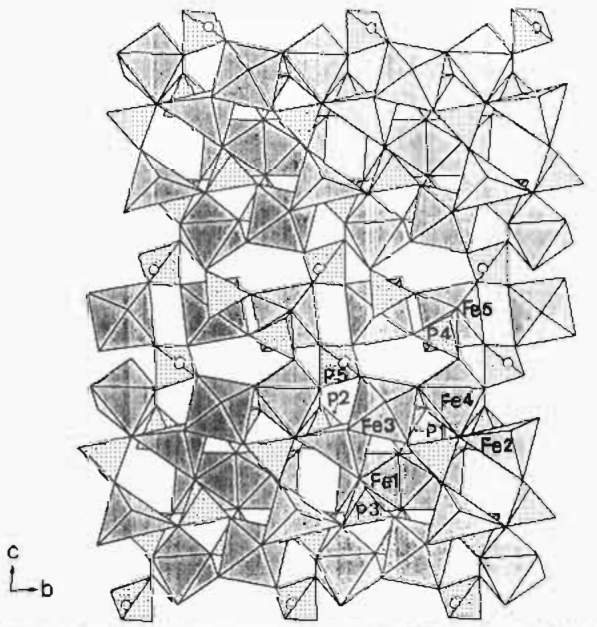

Figure 1. Polyhedral representation of the $CaFe_5(PO_4)_5(OH)\cdot H_2O$ structure along the [100] direction. Small open circles are Ca atoms.

Figure 2 presents the Schlegel diagrams[9] of the coordination polyhedra of the Fe atoms showing how the next-nearest neighbors are arranged in the structure. The Schlegel diagram has the advantage of pictorially representing a three-dimensional object

(8) Shannon, R. D. *Acta Crystallogr.* **1976**, *A32*, 751.

(9) Hoppe, R.; Koehler, J. Z. *Kristallogr.* **1988**, *183*, 77.

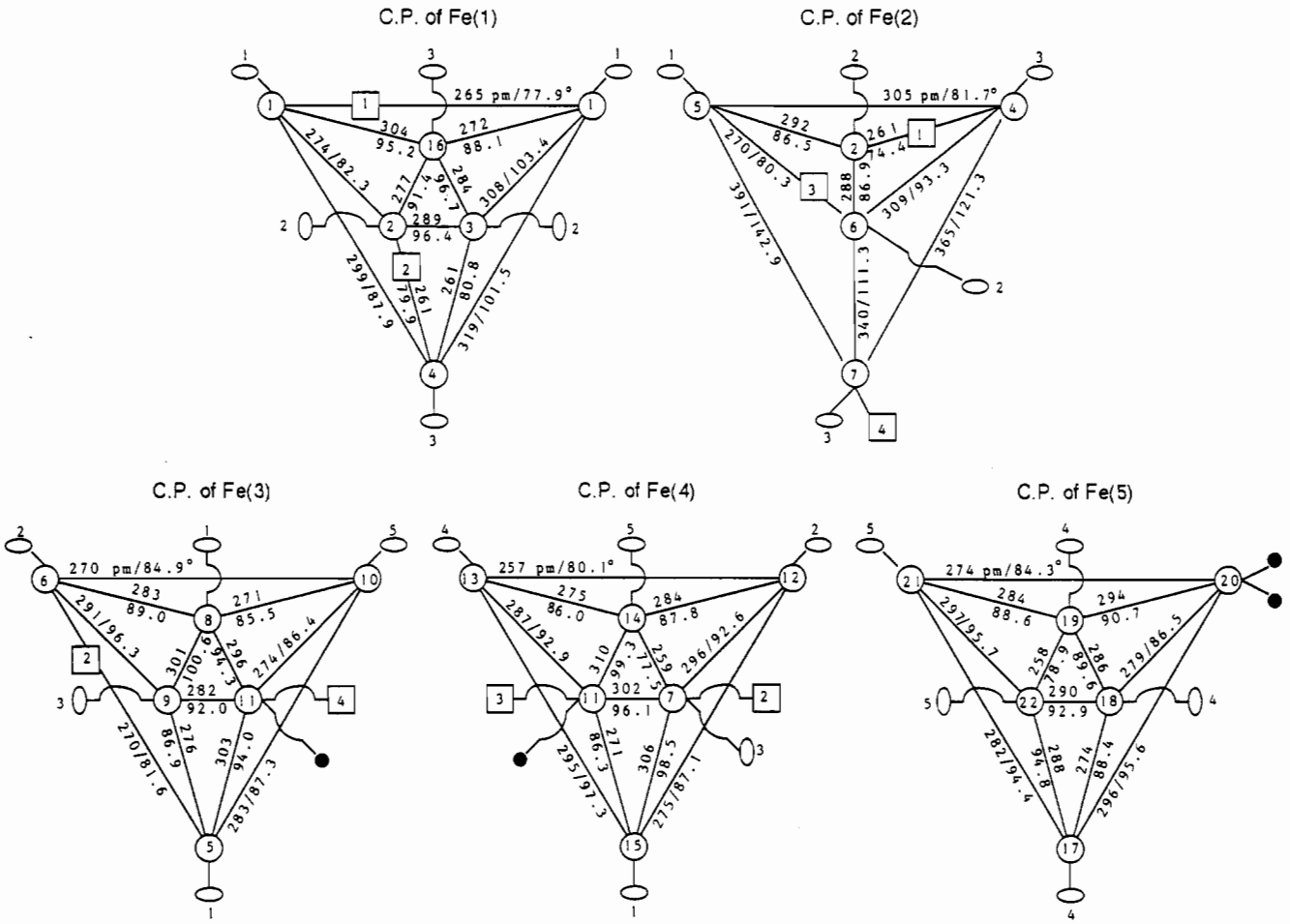

Figure 2. Schlegel projections of Fe–O polyhedra in $CaFe_5(PO_4)_5(OH)\cdot H_2O$. The central Fe atoms are not shown in the projections. The O···O distances (pm) and their corresponding angles (deg) with respect to the central atom are indicated next to the edges. Squares represent Fe atoms, ellipses represent P atoms, and small solid circles represent H atoms.

in two dimensions. It also offers the advantage over tables in that O···O distances and O–Fe–O bond angles can be inserted, easing the difficulty of relating tabular data to figures. Each FeO_5 trigonal bipyramid shares an edge with $Fe(1)_2O_{10}$, an edge with $Fe(3)Fe(4)(OH)O_{10}$, and a corner with another $Fe(3)Fe(4)(OH)O_{10}$. The shared edges of two Fe–O polyhedra are commonly short. The iron atoms are displaced from the centroids of their Fe–O polyhedra away from each other. The shortening of the shared edges is evidence that the structure is mainly ionic. The Fe···Fe distances are longer than 3.16 Å. From the Fe–O bond lengths, the O···O distances, and the O–Fe–O bond angles, we see that each polyhedron is markedly distorted. The octahedral distortion can be estimated by using the equation $\Delta = (1/6)\sum[(R_i - \bar{R}/\bar{R}]^2$, where R_i = individual bond length and $\bar{R}$ = average bond length.[8] The calculation results show that $Fe(1)O_6$ ($10^4 \times \Delta = 28$) is considerably more distorted than the others ($10^4 \times \Delta = 9.8$ for $Fe(3)O_5(OH)$, 4.4 for $Fe(4)O_5(OH)$, and 5.8 for $Fe(5)O_5(H_2O)$). The octahedral distortion is correlated with the number of shared edges. The Fe(3) and Fe(1) octahedra have one and two shared edges, respectively. The Fe(4) octahedron shares corners with two Fe octahedra and five phosphate tetrahedra. The Fe(5) octahedron shares corners with phosphate tetrahedra only. The coordination polyhedron of Fe(2) is in a geometry of distorted trigonal bipyramid with an average of Fe–O distance of 2.106 Å. Coordiation number 5 in iron phosphates is less common than number 6. As shown in Figure 3, the axial oxygens O(2) and O(6) bend away from the equatorial oxygen O(7) and the O(2)–Fe(2)–O(6) angle decreases to 161.7°. The structure is closer to trigonal bipyramid than to square pyramid. Bond-length bond-strength calculation indicates that Fe(2) is in the ferrous state, although high-spin Fe^{2+} gains slightly

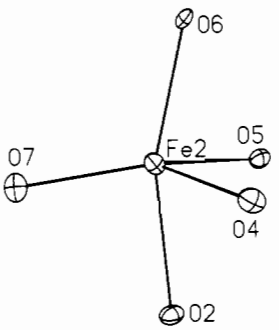

Figure 3. The coordination of oxygen atoms around an Fe(2) atom.

more crystal field stabilization energy by going into octahedral site than by occupying trigonal bipyramid site. A similar result was also observed in the mixed-valence compound $Fe_7(PO_4)_6$,[10] which contains Fe^{3+} in octahedral coordination and Fe^{2+} in either octahedral or trigonal bipyramid coordination. It should be noted that the ferrous atom Fe(2) in the title compounds has an additional (sixth) oxygen neighbor, O(14), at 2.524 Å in the Ca compound and at 2.621 Å in the Sr compound.

Mossbauer Effect Results. As shown in Figure 4, the room-temperature Mossbauer spectrum of $CaFe_5(PO_4)_5(OH)\cdot H_2O$ was least-squares fitted with three doublets with constraint on the area ratio of 1:1:3. A fit with unconstrained peak areas was also performed. All the spectral parameters are listed in Table IV. Components 2 and 3 have isomer shifts typical of Fe^{III}. The

(10) Gorbunov, Yu. A.; Maksimov, B. A.; Kabalov, Yu. K.; Ivashchenko, A. N.; Mel'nikov, O. K.; Belov, N. V. *Dokl. Akad. Nauk SSSR* **1980**, *254* (4), 873.

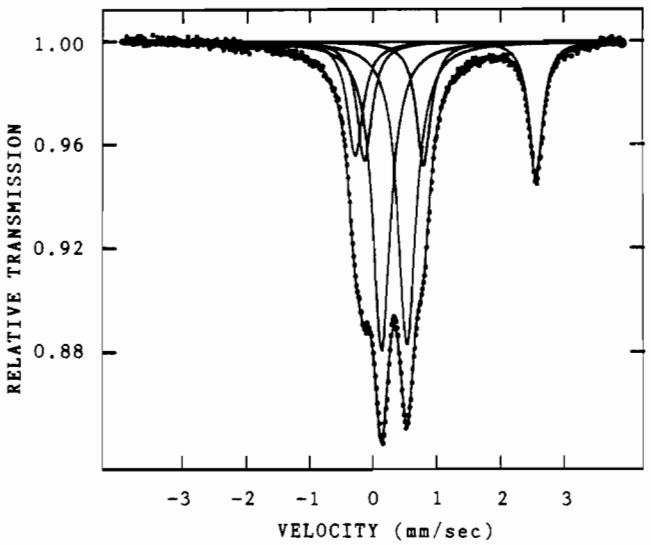

Figure 4. Mossbauer spectrum of $CaFe_5(PO_4)_5(OH)\cdot H_2O$ at 300 K. The fit is constrained so that the three components have an area ratio 1:1:3.

doublet with larger quadrupole splitting can be assigned to Fe(1), and the doublet with smaller quadrupole splitting, to Fe(3), Fe(4), and Fe(5). The octahedral Fe atoms have very different quadrupole splittings because their deviations from perfect octahedral symmetry are somewhat different. The octahedron around Fe(1) is considerably more distorted and it is likely to have larger quadrupole splitting. The octahedral distortions for Fe(3), Fe(4), and Fe(5) are comparable; consequently, component 3 can be assigned to them. Component 1 has a isomer shift characteristic of Fe^{II} and can be assigned to Fe(2). The isomer shifts for all three components are consistent with those for Fe^{III} and Fe^{II} compounds as compiled by Gleitzer.[11] Thus the Mossbauer spectrum confirms the presence of one Fe^{II} and four Fe^{III} in $CaFe_5(PO_4)_5(OH)\cdot H_2O$.

Table IV. Mossbauer Spectral Parameters (mm/s) for $CaFe_5(PO_4)_5(OH)\cdot H_2O$ at 300 K

	intensity ratio	δ^a	$\Delta E_Q{}^b$	Γ^c
component 1	1 (1)[d]	1.24 (1.25)	2.83 (2.82)	0.25, 0.30 (0.27, 0.32)
component 2	1 (1.12)	0.44 (0.44)	0.93 (0.90)	0.28, 0.29 (0.31, 0.35)
component 3	3 (2.56)	0.44 (0.44)	0.40 (0.39)	0.34, 0.34 (0.32, 0.32)

[a] Isomer shift (referred to iron). [b] Quadrupole splitting. [c] Full width at half-height. The width for the line at more positive velocity is listed first for each doublet. [d] The values in parentheses are taken from the fit with unconstrained peak areas.

The iron phosphate system has a rich crystal chemistry and contains a large number of new structural types. Their complex crystal structures are a challenge to complete characterization. Since hydrothermal methods have been successfully used in this system, it is likely that many more iron phosphates with novel frameworks will be forthcoming.

Acknowledgment. Support for this study by the National Science Council and Institute of Chemistry, Academia Sinica, of the Republic of China is acknowledged. The authors thank Dr. T.-Y. Dong and Mr. Y.-S. Wen for Mossbauer spectroscopy measurements and X-ray intensity data collection.

Supplementary Material Available: Tables giving crystal data and details of the structure determination, anisotropic thermal parameters, and bond distances and angles (14 pages). Ordering information is given on any current masthead page.

(11) Gleitzer, C. *Eur. J. Solid State Inorg. Chem.* **1991**, *28*, 77.